Diachronous metamorphism of the Ladakh Terrain at the Karakorum-Nanga Parbat-Haramosh junction (NW Baltistan, Pakistan)

Autor(en): **Villa, Igor M. / Ruffini, Raffaella / Rolfo, Franco**

Objekttyp: **Article**

Zeitschrift: **Schweizerische mineralogische und petrographische Mitteilungen = Bulletin suisse de minéralogie et pétrographie**

Band (Jahr): **76 (1996)**

Heft 2

PDF erstellt am: **24.04.2024**

Persistenter Link: https://doi.org/10.5169/seals-57701

SCHWEIZ. MINERAL. PETROGR. MITT. 76, 245–264, 1996

Diachronous metamorphism of the Ladakh Terrain at the Karakorum-Nanga Parbat-Haramosh junction (NW Baltistan, Pakistan)

by *Igor M. Villa*[1], *Raffaella Ruffini*[2], *Franco Rolfo*[3] and *Bruno Lombardo*[2]

Abstract

Metamorphic minerals from gneisses, amphibolites and schists of the Himalaya-Ladakh/Kohistan syntaxis in NW Baltistan were dated by $^{39}Ar/^{40}Ar$ stepwise heating.

The amphiboles from the Askore Amphibolite unit sampled in the Indus valley give discordant age spectra with step ages ranging from 35 to 70 Ma; we interpret the older step ages as mixtures between relict amphibole cores and new overgrowths. At least in the case of an amphibolite from the NW basal part of the Askore Amphibolite located just above the Main Mantle Thrust, a discordant age spectrum can be quantitatively interpreted using isotope correlations supplemented by petrographic observations and microprobe analyses. The cores retained their Ar during a 600–650 °C amphibolite facies overprint. In the Shyok Suture Zone, amphibole ages are much younger, between 9 and 14 Ma. The young radiometric ages are thought to be associated with new amphibole formation along the footwall of the Main Karakorum Thrust.

Three biotite ages from the Shyok Suture Zone range between 6 and 8 Ma, similar to that from the NW part of the Askore Amphibolite, while two biotites from the Askore Amphibolite further SE give ages around 35 Ma, very close to the coexisting hornblendes. Biotites from the "Layered Sequence" of the Nanga Parbat-Haramosh Massif contain excess Ar, as shown by comparing $^{39}Ar/^{40}Ar$ biotite ages (15 and 27 Ma) with muscovite $^{39}Ar/^{40}Ar$ ages (10–12 Ma) and a two-point biotite-plagioclase Rb–Sr age of 5.6 Ma. The Rb/Sr age may point to open-system fluid circulation and/or to Sr inheritance in plagioclase. The muscovites probably date the initial stages of the still-continuing formation of the Nanga Parbat-Haramosh Massif antiform.

The Askore Amphibolite underwent amphibolite metamorphism before 35–40 Ma, followed by rapid exhumation. The Karakorum Metamorphic Complex was thrust over the Shyok Suture Zone between 10–15 Ma, thermally overprinting it. One Askore Amphibolite sample from the basal part of the Ladakh Terrain records a Late Miocene thermal overprint related to the young high-grade metamorphism and penetrative deformation affecting the "Layered Unit" of the Nanga Parbat-Haramosh Massif.

Keywords: $^{39}Ar/^{40}Ar$-dating, amphibolite facies, tectonic evolution, exhumation, Ladakh, NW-Himalaya.

1. Introduction

The Himalaya-Ladakh/Kohistan syntaxis in Baltistan (Northern Pakistan) is divisible into three major geological units exposed south of the Karakorum Metamorphic Complex (KMC): the High Himalayan Crystallines of the Nanga Parbat-Haramosh Massif (NPHM), the Ladakh Terrain (LT) and a volcano-sedimentary unit, previously termed Greenstone Complex and included in the LT (Le Fort et al., 1995). Basing both on lithological comparison between our rocks and the Shyok type locality (Thakur, 1993, and references therein) and on the petrological and chronological differences between the volcano-sedimentary unit and the LT shown by the present work, we now propose that this unit be identified as a NW extension of the Shyok Suture Zone (SSZ), which separates the Ladakh Terrain to the S from the Karakorum to the N.

[1] Laboratorium für Isotopengeologie, Mineralogisch-Petrographisches Institut, Universität Bern, Erlachstrasse 9a, CH-3012 Bern, Switzerland. E-mail: igor@mpi.unibe.ch.
[2] CS Geodinamica Catene Collisionali, CNR, via Valperga Caluso 35, I-10125 Torino, Italy.
[3] Dip. Scienze Mineralogiche e Petrologiche, Università degli Studi di Torino, via Valperga Caluso 35, I-10125 Torino, Italy.

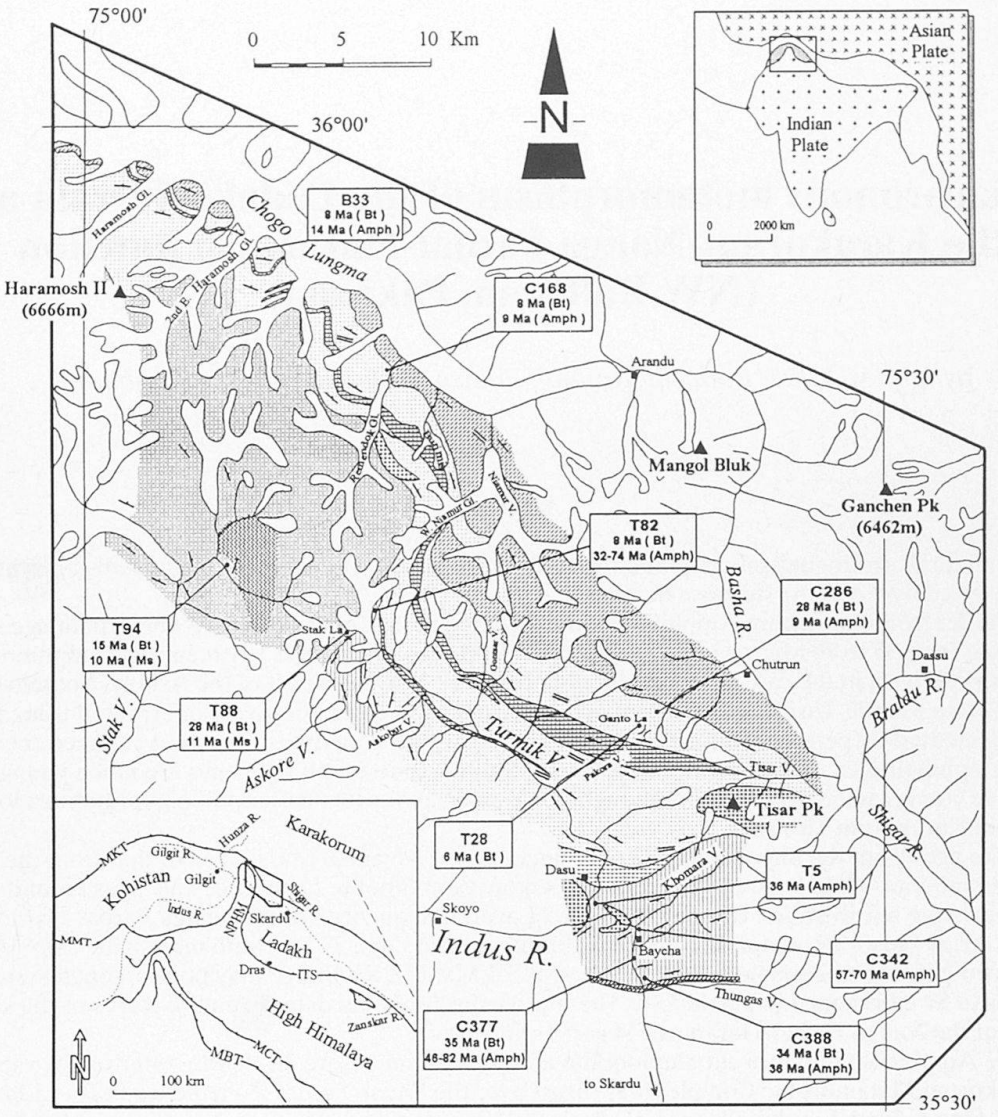

KARAKORUM

Undifferentiated metasediments

SHYOK SUTURE ZONE

Metasedimentary and metavolcanic sequences

Pakora and other limestones

Dasu Ultramafic

trends of regional foliation

LADAKH TERRAIN

Askore Amphibolite

Thungas marble

Skoyo, Tisar and Gontsar plutons

Remendok Leucotrondhjemite

NANGA PARBAT-HARAMOSH MASSIF

Banded Grt-Ky-Bt gneiss

Granitic orthogneiss

Fig. 1 Outline geological map of the junction between the High Himalayan Crystallines of the Nanga Parbat-Haramosh massif, the Shyok Suture Zone, the Ladakh Terrain, and the Karakorum Metamorphic Complex in the Chogo Lungma to Turmik area, modified after LE FORT et al. (1995), showing locations of geochronological samples. All the geological limits are tectonic contacts, except those of the Skoyo, Tisar and Gontsar plutons and of the Remendok leucotrondhjemite. Inset: tectonic sketch map of the NW Himalaya and Karakorum, showing the regional setting of the investigated area. Acronyms are: NPHM, Nanga Parbat-Haramosh massif; MKT, Main Karakorum Thrust; MMT, Main Mantle Thrust; ITS, Indus-Tsangpo Suture; MCT, Main Central Thrust; MBT, Main Boundary Thrust. Mineral abbreviations are after KRETZ (1983).

The geochronology of the Himalaya-Ladakh/Kohistan syntaxis is conventionally interpreted in terms of an Eocene metamorphic peak with subsequent Oligo-Miocene cooling (ZEITLER, 1985).

A prominent morphologic feature is the Nanga Parbat (8125 m) – Haramosh (7409 m) Massif, which was the site of spectacular Pleistocene vertical movements and Mio-Pliocene cooling (ZEITLER, 1985; see below for further discussion).

Tectonic analysis of the Nanga Parbat fold (TRELOAR et al., 1991) suggested that it has grown above the pinned lateral termination of a major Himalayan thrust, possibly the Main Central Thrust. From this interpretation, the NPHM would not be structurally unique and other areas of recent exhumation further to the north and east may be expected.

Late Miocene cooling ages were repeatedly reported in the literature also for the Karakorum Metamorphic Complex (SEARLE et al., 1989, and references therein; cfr. also VILLA et al., 1996) but their relations to the young metamorphism and Pliocene exhumation of the NPHM are not yet fully appreciated.

Recent geochronological work on the Karakorum Metamorphic Complex of the Chogo Lungma-Basha area discovered an intense tectonometamorphic event as young as Pliocene near Hemasil in the Basha valley, and a very young intrusive body sealing the contact between the NPHM and the LT (VILLA et al., 1996). The purpose of the present paper is to investigate the regional age pattern of the tectonic units of the syntaxis (the High Himalaya Crystallines of the NPHM, the SSZ and the LT) in an area mid-way between the two localities with known Pliocene cooling, the Basha valley and the Indus gorge south and west of Haramosh (Fig. 1).

2. Geological setting

2.1. NANGA PARBAT-HARAMOSH MASSIF

The NPHM is a major, north-trending antiformal structure oblique to direction of thrusting in the NW Himalaya. Uplift of the NPHM antiform has interrupted the lateral continuity of the Ladakh-Kohistan Terrain, resulting in a tectonic half-window which exposes deep parts of the leading edge of the Indian plate. Its formation has been ascribed to laterally inhibited SSE-directed thrusting (COWARD et al., 1986).

The rocks of the northern NPHM are polymetamorphic para- and orthogneisses of high metamorphic grade, hosting a suite of basic sheets metamorphosed in the amphibolite facies during the Himalayan cycle (WHEELER et al., 1995). According to MADIN (1986) two sub-units can be recognized in the area north of the Indus river, the Iskere orthogneiss to the west and the Shengus paragneiss, imbricated with minor orthogneiss, to the east. The Shengus Gneiss is interpreted by TRELOAR et al. (1991) as being a cover to the Iskere Gneiss and tentatively correlated with the Tanawal Formation – Mansehra Granite series of the Hazara region (Lower Himalayan nappes of Pakistan).

Another lithological unit is found at the top of the Phuparash and Mani valleys, the "Layered Unit" (BUTLER et al., 1992). This unit is the northernmost and structurally highest lithological unit of the NPHM, cropping out just below the Main Mantle Thrust. Lithologies exposed east of Haramosh in the middle and upper Stak valley and in the uppermost Turmik valley appear to be correlatives of the "Layered Unit", as they are in physical continuity with it and match well the lithologies found by BUTLER et al. (1992) in the headwalls of the Phuparash and Mani glaciers. In the upper Stak valley the dominant lithologies are strongly foliated biotite-muscovite-garnet-kyanite gneiss, granitic biotite-muscovite-garnet-kyanite orthogneiss and foliated garnet-kyanite leucogranites (ZANETTIN, 1964; POGNANTE et al., 1993; LOMBARDO, ROLFO and VISONÀ, in prep.). Like in the Shengus and Iskere gneisses, metabasic sheets also occur in the gneiss of the Stak valley, but they are metamorphosed in the garnet-granulite facies (POGNANTE et al., 1993). Subvertical, undeformed leucogranite sheets crosscutting the metamorphic (blastomylonitic) foliation of the Stak gneiss were found in the upper Stak and Turmik valleys by POGNANTE et al. (1993).

Lithologically series similar to those of the Stak valley also crop out at the top of several southern tributaries of Chogo Lungma Glacier (LE FORT et al., 1995). For these rocks, ROLFO et al. (1995) proposed an early compressional evolution from the sillimanite to the kyanite stability field, followed by decompressional cooling in the kyanite field. The garnet-granulite assemblage in the basic dikes constrains the metamorphic peak at T = 650–700 °C (geothermometers of POWELL, 1985; KROGH, 1988) and P = 12–15 kbar (geobarometers of HOLLAND, 1980; NEWTON and PERKINS, 1982; POWELL and HOLLAND, 1988). Similar P-T values were obtained on rocks from the "Layered Unit" in the Stak valley by POGNANTE et al. (1993).

2.2. THE MAIN MANTLE THRUST ZONE

The Main Mantle Thrust (MMT), a major thrust zone which connects southwards to the Indus Su-

ture Zone, separates the Indian plate gneisses of the NPHM from the overlying LT. The MMT can be followed from the Astor valley in the south (CASNEDI and EBBLIN, 1977) through the Askore valley (ZANETTIN, 1964) and the upper Turmik valley (POGNANTE et al., 1993) to the S side of Chogo Lungma Glacier (LE FORT et al., 1995) (Fig. 1). According to Verplanck et al. (1985), the eastern margin of the NPHM is an east-side down normal fault (the Stak fault) which cuts out the MMT. This interpretation is not supported by the observations of TRELOAR et al. (1991) along the Indus gorge, where no evidence was found "that the MMT is significantly deformed or reworked other than having undergone an essentially passive steepening on the limb of the major north-trending fold". Along both sides of Remendok valley, a southern tributary of Chogo Lungma Glacier, the MMT was seen to be sealed by the intrusion of the Remendok Leucotrondhjemite (LE FORT et al., 1995), which was emplaced at about 10 Ma (VILLA et al., 1996).

2.3. LADAKH TERRAIN

The LT is the remnant of a Cretaceous island arc (TAHIRKHELI et al., 1979; BARD et al., 1980; DIETRICH et al., 1983). In the area east of the NPHM, the LT consists of the Ladakh-Deosai batholith and, north of it, of the Askore Amphibolite (AA) and other small intrusive bodies (Skoyo, Twar, etc.). On lithological and structural grounds the AA appears a correlative of the Chalt Volcanics of Cretaceous age exposed W of the NPHM in the Hunza valley. Both these units comprise a sequence of lavas and volcanoclastics; in the Chalt Volcanics they vary in composition from high-Mg basalt and andesite to low-Mg basalt, andesite and rhyolite (PETTERSON et al., 1991).

In the Askore canyon and in upper Turmik valley, close to the contact with the underlying NPHM, the AA consists of massive garnet-epidote-andesine amphibolite and epidote-oligoclase-clinozoisite amphibolite. The metamorphic facies of AA in this area is typically high-P amphibolite. The metamorphic peak assemblage defines the regional foliation and apparently equilibrated at T = 600–650 ° C and P = 10 kb (ROLFO et al., 1995, and in prep.).

In the Indus valley, the Askore meta-volcanic sequence is represented by epidote amphibolites with concordant layers of saccharoidal marbles (south of Thungas), hosting both concordant and discordant dykes of tonalite to granodiorite and trondhjemite. These are related to the plutonic bodies of Skoyo and Twar. The Skoyo pluton (Skoyo gneiss of ZANETTIN, 1964), consists of a rim of basic agmatite and a core of foliated trondhjemite and tonalite which reaches the Indus-Turmik divide west of lower Turmik valley. The Twar pluton is exposed along the Indus valley N of Rondu. The most voluminous rocks in the Twar pluton are hypersthene-bearing diorite and norite, with minor quartzdiorite and pyroxene-bearing biotite-amphibole granodiorite (ZANETTIN, 1964; VERPLANCK, 1986). In the western margin of the pluton these rocks are transformed into variably foliated metadiorite and metanorite (ZANETTIN, 1964). Foliated meta-tonalite and granodiorite, presumed to derive from this structural level occur in the moraine material of the Haramosh Glacier and other southern tributaries of the Chogo Lungma Glacier to the E.

The AA in the Indus valley section between the mouth of the Turmik river and Thungas is typically in medium-P amphibolite facies. The metamorphic peak assemblage defines the regional foliation and is overprinted by a later static recrystallization at T = 600–650 °C and P = 5–6 kb.

Along the Indus valley from Skardu to Thungas the LT is represented by the Katzarah Formation, a calc-schist and granofels with rare pelitic horizons (ZANETTIN, 1964; HANSON, 1989; ALLEN and CHAMBERLAIN, 1991), occupying the core of a large, open antiform. Both lithologically and structurally, the Katzarah Formation is similar to the Gilgit Gneiss (KHAN, 1994) occurring in the Kohistan Terrain north of the Kohistan Batholith. The Katzarah Formation is separated from the Ladakh-Deosai Batholith by the Burji Formation (DESIO, 1978), consisting of black slates, fossiliferous limestones of Turonian age and andesitic sills and lenses, and showing the lowest metamorphic grade of the whole Skardu area.

2.4. SHYOK SUTURE ZONE

In the lower Turmik valley, the AA is separated from the low-grade metasedimentary rocks of the overlying SSZ by the Dasu Ultramafic, a lenticular body of antigorite-bearing metaperidotite, 5 × 2 km, in which a relict cumulitic structure is still recognized (LE FORT et al., 1995). A screen of rodingite (tremolite-talc-carbonate-epidote fels) divides the Dasu Ultramafic from the Cretaceous volcano-sedimentary series of the SSZ. Similar bodies of cumulitic metaperidotite surrounded by calc-silicate rocks crop out at different tectonic levels of the SSZ near lower East Marpho Glacier and in Remendok valley, S of Chogo Lungma Glacier.

On both sides of Turmik valley, blastomy-

lonitic arenaceous slates are the strucurally lowest member of the SSZ volcano-sedimentary series (Turmik Formation of DESIO, 1963). This, however, does not correspond to a stratigraphic sequence because of isoclinal folding and internal shearing. Along the N side of Turmik valley, the rocks are quartz-albite-epidote-chlorite-carbonate arenaceous slates and conglomeratic schists more or less rich in micaceous matrix, with minor intercalations of amphibole schists (ZANETTIN, 1964; LE FORT et al., 1995). The clasts of the conglomeratic schists consist of acid to intermediate volcanics, together with minor amphibolite and serpentinite. The uppermost member of the Turmik series is a more than 100 m thick sheet of light green quartz-plagioclase-muscovite-chlorite-biotite-epidote phyllite with large rombohedral crystals of carbonate and, more sporadically, also of low-iron epidote. Kyanite and chloritoid occur in metasedimentary rocks of the SSZ (LE FORT et al., 1995). Overall, metamorphic grade in the SSZ appears to increase from greenschist facies to amphibolite facies, moving westwards to the deeper structural levels exposed at the tip of the NPHM and northwards towards the KMC.

A thick band of meta-limestone, partly conglomeratic (Munbluk Limestone of DESIO, 1963; Pakora Limestone of LE FORT et al., 1995) with black shale layers and fossils of Valanginian age (LE FORT et al., 1995), separates the Turmik Formation from a mélange-like unit, the Blanzgo Formation of DESIO (1963), consisting of metavolcanic rocks (amphibole-epidote-biotite greenschists), with minor plagioclase-biotite-epidote schists, phyllitic calcschists and serpentinite lenses. North of Ganto La a band of meta-limestone with strongly folded intercalations of black schist with biotite porphyroblasts separates the Blanzgo Formation from the highly recrystallized Chutrun meta-limestone, the southernmost member of the KMC.

2.5. KARAKORUM METAMORPHIC COMPLEX

The geology of the KMC in the Basha-Chogo Lungma area is described by LEMENNICIER et al. (1995). Granite to tonalite orthogneisses and metasedimentary lithologic series record two main tectonometamorphic events. The first event (D1) is characterized by N110°E south-vergent isoclinal folds associated with an axial-plane cleavage and garnet-biotite-muscovit-kyanite assemblages in metasedimentary lithologies. West of the Basha valley, metasedimentary lithologic members contain staurolite instead of kyanite. Metamorphic peak conditions for the D1 event are T = 620–730 °C , P = 7.5–11 kbar. The second event (D2) is a fast, nearly isothermal decompression in the sillimanite field with a P decrease from more than 7.5 kbar down to 4 kbar and only slight changes in T. Structurally, it corresponds to the development of conical domes elongated N110–140°E, which are the major structures in the KMC from Chogo Lungma to the Biafo Glacier.

$^{39}Ar/^{40}Ar$ dating on biotite, muscovite and amphibole related to the D2 event (VILLA et al., 1996) give very young cooling ages between 8 and 3.5 Ma, suggesting that doming in the KMC occurred at the Miocene-Pliocene boundary and denudation rates in the area have since remained high.

3. Sample description

Eleven samples where chosen for geochronological analysis on the basis of their geographical position and lack of alteration: two samples of metapelitic gneiss from the HHC of the NPHM, five samples of amphibolite and amphibole gneiss from the AA, three samples of amphibole gneiss and one sample of biotite calc-schist from the SSZ.

The area of provenance is a rectangle, approximately 20 × 50 km in size, covering the area from the north-eastern tip of the NPHM to the Indus gorge halfway between Skardu and Rondu (Fig. 1). Two samples belong to the upper structural levels of the NPHM (T88 and T94), one to the lowermost structural levels of the AA, just above the MMT (T82), four to the AA of the Indus valley (T5, C342, C377, C388) and four to the uppermost part of the SSZ close the KMC (B33, C168, C286 and T28).

Minerals of these samples have been analyzed using an EDS/SEM microprobe. Representative compositions are reported in table 1 and discussed below.

3.1. NANGA PARBAT-HARAMOSH MASSIF

T88 is a two mica-garnet-kyanite gneiss, collected at 4400 m elevation on the western side of Stak La. The equilibrium assemblage is quartz-K-feldspar-oligoclase-garnet-biotite-kyanite-muscovite-rutile, with a small amount of chlorite as alteration product. The metamorphic foliation is defined by red biotite, muscovite and kyanite, which are often concentrated in mm-thick layers wrapping around K-feldspar and garnet porphyroclasts. Biotite of the same composition is also found in pressure shadows of garnet.

Tab. 1 Representative microprobe analyses of amphiboles and biotites from the Chogo Lungma – Turmik area of Baltistan. Structural formulae are calculated on the basis of 7 cations and 12 oxygens for biotite and 13 cations and 23 oxygens for amphibole. Fe^{3+} in amphibole is estimated assuming the total cation content – (Ca + Na + K) = 13. B33, C168, C286: Shyok Suture Zone. T82: Askore Amphibolite just above the MMT. T5, C377,C388: Askore Amphibolite of the Indus Valley.

	AMPHIBOLE							BIOTITE						
	B33	C168	T82	C286	T5	C377	C388	B33	Ct168	T82	T28	T5	C377	C388
SiO_2	44.15	44.67	43.26	42.74	46.91	41.45	45.25	38.53	39.32	37.84	39.05	38.56	37.73	39.77
TiO_2	0.63	0.33	0.19	0.56	0.46	0.99	0.49	2.10	2.29	1.61	1.51	1.94	2.51	2.37
Al_2O_3	15.49	16.23	15.47	15.71	11.21	15.11	12.30	17.13	17.59	16.23	19.25	17.23	17.50	17.55
FeO^{tot}	15.54	12.57	16.84	16.22	12.74	19.27	14.54	15.47	13.71	17.04	14.77	12.57	19.25	13.21
MnO	0.26	0.14	0.32	0.32	0.22	0.14	0.28	0.08	0.04	0.02	0	0.11	0.40	0.01
MgO	8.92	10.04	8.59	8.93	12.82	6.61	11.33	12.63	13.95	13.72	12.29	15.32	9.32	13.10
CaO	10.58	11.28	10.70	10.76	11.28	10.90	11.17	0.46	0.31	0.06	0.24	0.05	0.51	0.54
Na_2O	2.54	1.95	2.15	1.75	1.75	2.31	2.24	0.61	0.20	0.40	0	0.61	0	0.63
K_2O	0.36	0.49	0.61	0.66	0.26	1.15	0.52	8.44	8.92	9.47	9.13	9.25	9.17	8.76
H_2O	2.06	2.07	2.01	2.02	2.08	1.99	2.05	3.94	4.03	3.97	4.13	4.01	3.93	3.97
Total	100.58	99.77	100.14	99.67	99.73	99.92	100.17	99.39	100.36	100.36	100.37	99.86	100.32	99.92
Sl	6.419	6.478	6.384	6.255	6.794	6.260	6.615	2.928	2.926	2.813	2.842	2.878	2.825	2.999
Al^{IV}	1.581	1.522	1.616	1.745	1.206	1.740	1.385	1.072	1.074	1.188	1.158	1.122	1.175	1.001
Al^{VI}	1.073	1.251	1.074	0.965	0.707	0.948	0.733	0.462	0.469	0.234	0.493	0.394	0.370	0.559
Ti	0.074	0.036	0.021	0.062	0.050	0.113	0.054	0.120	0.128	0.091	0.082	0.109	0.141	0.134
Fe^{3+}	0.284	0.052	0.245	0.673	0.226	0.144	0.313	–	–	–	–	–	–	–
Fe^{2+}	1.604	1.472	1.805	1.312	1.291	2.290	1.397	0.983	0.853	1.060	0.898	0.785	1.205	0.833
Mn	0.032	0.018	0.040	0.040	0.027	0.017	0.034	0.005	0.003	0.001	0	0.007	0.025	0.001
Mg	1.932	2.170	1.880	1.949	2.766	1.489	2.468	1.431	1.548	1.521	1.332	1.705	1.041	1.473
Ca	1.647	1.753	1.691	1.687	1.750	1.763	1.750	0.037	0.024	0.005	0.018	0.004	0.041	0.044
Na	0.353	0.247	0.309	0.313	0.250	0.237	0.250	0.090	0.028	0.057	0	0.118	0	0.092
Na	0.363	0.302	0.306	0.184	0.241	0.439	0.385	–	–	–	–	–	–	–
K	0.067	0.090	0.115	0.112	0.048	0.221	0.097	0.818	0.847	0.898	0.847	0.881	0.876	0.843

T94 is a fine-grained two-mica paragneiss collected at 3730 m elevation in the Goropha valley (upper Stak valley), just above the junction with Lecho Nala (see Fig. 1 and the topographic 1:100.000 map in LOMBARDI, 1991). The equilibrium assemblage is quartz-oligoclase-garnet-biotite-muscovite-kyanite K-feldspar, with tourmaline (concentrated in a single layer) and rutile as accessory phases. Unaltered red biotite and muscovite are in equilibrium and define the metamorphic foliation. Post-kinematic xenoblastic garnet includes all the other phases. The mineral chemistry of these gneisses has been studied by POGNANTE et al. (1993). Biotites have slight irregular zoning (X_{Mg} = 0.43–0.69). Muscovites have relatively low celadonite contents (Si = 3.13 atoms per 12 oxygens) and moderate to high X_{Mg} (0.51–0.73).

Equilibration temperatures and pressures in the NPHM rocks of the Stak and Turmik valleys were estimated by POGNANTE et al. (1993) combining different garnet-biotite thermometers (HODGES and SPEAR, 1982; PERCHUK and LAVRENT'EVA, 1983; INDARES and MARTIGNOLE, 1985) with different geobarometers (NEWTON and HASELTON, 1981; HODGES and CROWLEY, 1985; KOZIOL and NEWTON, 1988). Estimated peak temperatures range from 650 to 700 °C and pressures from 8 kbar to 13 kbar. Equilibration temperatures for garnet cores and included biotites are higher than for garnet rims and matrix biotites, suggesting retrograde Fe/Mg exchange and diffusion zoning during cooling.

3.2. ASKORE AMPHIBOLITE OF TURMIK VALLEY

T82 is a banded medium-grained amphibolite cropping out a few metres above the MMT in the upper Turmik valley at 4540 m elevation (see Fig. 1, and POGNANTE et al., 1993, Fig. 2). The equilibrium assemblage is hornblende-plagioclase (oligoclase-andesine)-epidote-biotite-quartz, with pyrite-rutile-ilmenite-apatite as accessory phases. The amphibolite has a gneissic texture defined by the orientation of deep greenish blue hornblende and brownish-green biotite, while feldspar- and quartz-rich layers with no amphibole and lesser amounts of biotite and epidote have a granoblastic polygonal texture. The amphibole (Tab. 1) is a tschermakitic hornblende (following the nomenclature of LEAKE, 1978) with X_{Mg} = 0.51. Hornblende grains show relict cores crowded with very small (~ 20 μm) needles of rutile and ilmenite, and rims of inclusion-free hornblende. Both rims and cores are tschermakitic in composition. The cores have higher Al^{VI} and represent higher-temperature amphibole compositions than the rims when the Ti exsolved as rutile/ilmenite is re-integrated; they may possibly be relics of magmatic hornblende. Neither of these two amphiboles is notably zoned. Si content is relatively high (6.38–6.22 atoms per 13 cations from core to rim) and Ti content is very low to moderate (0.02–0.07 atoms from core to rim), Al^{IV} and Al^{VI} vary in the range of 1.61–1.75 (core to rim) and 1.07–0.86 (core to rim) atoms per 13 cations, respectively (Fig. 2); X_{Mg} ranges around 0.5. Biotite is homogeneous, as shown by the absence of alteration at microscopic scale and by a nearly constant concentration for the major elements (Si = 2.81–2.86 atoms per 11 oxygens; X_{Mg} = 0.58–0.59).

3.3. ASKORE AMPHIBOLITE OF THE INDUS VALLEY

T5 is a fine grained epidote-biotite amphibolite intruded by a tonalite body of the Ladakh Plutons (see ROLFO et al., 1995), cropping out at 2400 m elevation at the mouth of Turmik valley. The equilibrium assemblage is pale greenish blue horn-

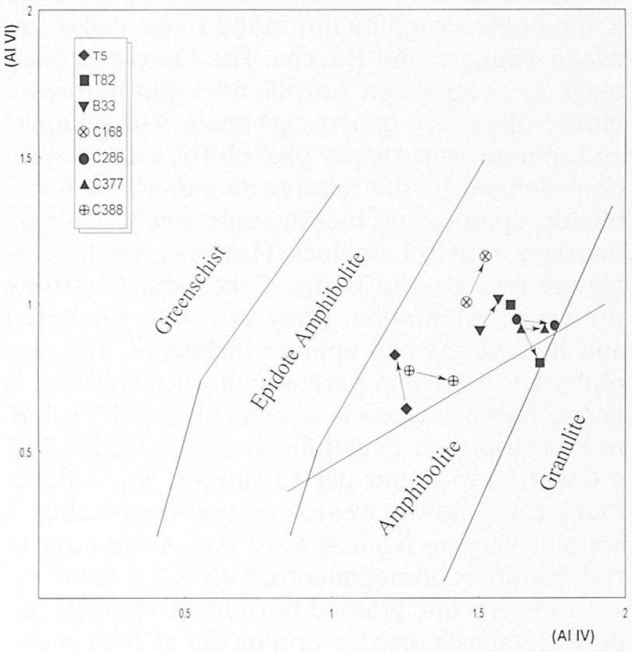

Fig. 2 Al^{VI} versus Al^{IV} diagram for amphiboles from samples T5, T82, B33, C168, C286, C377, C388. The gently sloping line separating low Al^{VI} (low pressure) from high Al^{VI} (high pressure) amphibole compositions is after RAASE (1974). The compositional fields of amphiboles from the greenschist facies, epidote-amphibolite facies, amphibolite facies and granulite facies are from the compilation of ZAKRUTKIN (1968). Arrows point from core to rim compositions.

blende-oligoclase-epidote-biotite-quartz, with rutile-ilmenite-sphene-apatite-zircon as accessory phases. The gneissic fabric is defined by the preferred orientation of the amphibole which in places forms small elongated aggregates, together with minor amounts of epidote and/or biotite. The amphibole shows a composition between Mg-hornblende and tschermakitic hornblende and is slightly zoned, with Al^{IV} decreasing from core to rim from 1.40 to 1.25 atoms per 13 cations, and Al^{VI} increasing from 0.60 to 0.72 atoms per 13 cations. X_{Mg} is 0.68 on average. Very small needles of rutile and ilmenite occur sometimes inside the amphibole cores. Brown-reddish biotite, though fresh, is occasionally weakly deformed and very subordinated in quantity, compared to amphibole. Biotite is quite homogeneous in composition (Si = 2.81–2.86 atoms per 11 oxygens; X_{Mg} = 0.66–0.69).

C342 is a hornblende rock occurring as large blocks north of Baycha village. The mineral assemblage is bluish hornblende with very minor amounts of biotite-epidote-rutile-Mg-chlorite-apatite. Amphibole crystals are fresh and up to 1 cm in size; they include small oriented biotite flakes, together with epidote and rutile. Somewhere, inclusions of very small oriented rutile needles occur. Pale red biotite, though unaltered, is quite small and infrequent.

C377 is a fine grained banded epidote-biotite amphibolite, cropping out in the Indus valley between Thungas and Baycha. The mineral assemblage is deep green hornblende-epidote-brown biotite-oligoclase-quartz-carbonate, with opaques and sphene as accessory phases. The gneissic fabric is defined by the relative abundance of hornblende, epidote and biotite respectively, in single interlayers up to 1 cm thick. However, small hornblende crystals and biotite flakes show a strong preferred orientation. They are both unaltered and host very small epidote inclusions. The amphibole is a ferroan pargasitic hornblende and is nearly homogeneous in composition (Al^{IV} = 1.66 to 1.74 atoms per 13 cations from core to rim; Al^{VI} = 0.94 to 0.95 atoms per 13 cations; X_{Mg} = 0.39). Plagioclase shows a weak reverse zonation, the Ca content varying from An_{20} to An_{26} from core to rim. Biotite is homogeneous, with X_{Mg} = 0.46.

C388 is a fine grained hornblende-biotite-epidote metabasic schist, cropping out at 2400 m elevation at the bottom of lower Thungas valley. The equilibrium parageneses is oligoclase-bluish green hornblende-brown biotite-epidote-quartz, with sphene-ilmenite-carbonate-zircon as accessory phases. The gneissic fabric is defined by the preferred orientation of hornblende and biotite. Plagioclase (ranging in composition from An_{33} to An_{21} from core to rim), epidote and minor quartz in the ground mass show a granoblastic texture. Amphibole, which is a Mg-hornblende with X_{Mg} = 0.64, shows a significant increase in Al^{IV} (1.20–1.41) from core to rim; it occurs also as crystals of the same composition, several mm long, which occasionally cross-cut the metamorphic foliation. Epidote, plagioclase and quartz inclusions are common inside the amphibole. Small elongated aggregates of hornblende and biotite are also present, the biotite showing a homogeneous composition (Si = 2.95–3.00 atoms per 11 oxygens; X_{Mg} = 0.63–0.64).

3.4. SHYOK SUTURE ZONE

B33 is a banded amphibolite collected at 4050 m elevation at the south-eastern side of Second East Haramosh Glacier. It is typified by the assemblage plagioclase-hornblende-biotite-quartz-epidote-tourmaline (a single layer), with ilmenite-titanite-apatite as accessory phases. Rare oligoclase relics are rimmed by newly grown albite. Brownish-green biotite with Si = 2.92–2.96 atoms per 11 oxygens and X_{Mg} = 0.59 (Tab. 1) defines the metamorphic foliation and is rarely altered into chlorite, whereas the fine-grained granoblastic matrix is mainly albite-oligoclase and quartz together with minor epidote. Porphyroblasts of greenish blue amphibole, locally slightly broken, have grown syn- to post-kinematic on the foliation. These porphyroblasts have a tschermakitic hornblende composition with X_{Mg} = 0.55 and show a light compositional zoning (both Al^{IV} and Al^{VI} increase from core to rim, see Fig. 2). The amphibole porphyroblasts are crowded by inclusions of epidote grains up to 0.1 mm long, quartz and plagioclase.

C168 is a fine-grained amphibolite cropping out a few hundred meters south of the contact between SSZ and KMC at 3700 m elevation, on the western side of lower Remendok valley. The equilibrium assemblage is greenish blue hornblende-oligoclase-quartz-biotite-epidote, with rutile-ilmenite-apatite as accessory phases. Plagioclase occurs as small crystals without any preferred orientation; a weak but persistent reverse zoning occur, with compositions ranging from An_{21} (core) to An_{28} (rim). The amphibole is a tschermakitic hornblende with X_{Mg} = 0.60 and shows compositional zoning (both Al^{IV} and Al^{VI} increase from core to rim, Fig. 2). Elongated amphibole clasts, often broken, are slightly altered to chlorite and Fe-carbonate. Brown-red biotite hosts a few epidote and rutile crystals, and has the same composition (Si = 2.92–2.98 atoms per 11 oxygens; X_{Mg} = 0.63–0.66, Tab. 1) both on the foliation and in microlithons.

C286 is a hornblende-biotite schist cropping out at 3780 m elevation at the northern side of Matunturu valley, 1 km north-east of Ganto La. It is characterized by the assemblage oligoclase-quartz-greenish blue hornblende-Fe-carbonate-Mg-chlorite-epidote-biotite-rutile-ilmenite-titanite-apatite. Brownish biotite, though unaltered, is weakly deformed and defines the metamorphic foliation, together with chlorite flakes wich are in equilibrium with biotite. Green amphibole is a tschermakitic hornblende and occurs as porphyroblasts which are both concordant and discordant to the foliation, but have the same, slightly zoned composition with X_{Mg} = 0.60, increasing Al^{IV} and decreasing Al^{VI} from core to rim (from 1.56 to 1.75 and from 1.01 to 0.86 atoms per 13 cations, respectively). Small inclusions of epidote, plagioclase and quartz are common in the hornblende porphyroblasts. Plagioclase crystals, both as inclusions and in the ground-mass, show a weak reverse zoning from An_{20} (core) to An_{30} (rim).

T 28 is a graphitic calc-schist with biotite porphyroblasts, collected at ca. 4000 m elevation in the Pakora valley, just west of Ganto La. The equilibrium assemblage is pale reddish brown biotite-white mica-carbonate-quartz-graphite-clinozoisite-ilmenite. Very fine grained white mica and biotite define the metamorphic foliation, while up to 5 mm large biotite porphyroblasts grow syn- to post-tectonic. Biotite porphyroblasts are unaltered and homogeneous in composition (average Si = 2.84 atoms per 11 oxygens and X_{Mg} = 0.60, Tab. 1) and host small quartz and clinozoisite grains, together with very fine grained graphite.

4. Geochronology

We analyzed nine biotites, eight amphiboles and two muscovites by $^{39}Ar/^{40}Ar$ stepwise heating and one plagioclase-biotite pair by the Rb/Sr method. For eight rocks we obtained age data on at least two geochronometers. Samples were irradiated in the TRIGA reactor in Pavia and heated in a double-vacuum resistance furnace. Ar was analyzed in a MAP® 215-50B rare gas mass spectrometer, Rb and Sr in a VG® 354 solid source mass spectrometer. $^{39}Ar/^{40}Ar$ results are summarized in table 2 and visualised in figures 3–6, Rb/Sr results are given in table 3. The full analytical data are available from the authors.

4.1. NANGA PARBAT-HARAMOSH MASSIF

Two-mica gneiss *T94* is shown in figures 3 a–b. This sample comes from the inner part of the antiform.

Tab. 2 Summary of Ar–Ar data. Units to which samples are assigned: S = Shyok Suture Zone; A = Askore Amphibolite of the Turmik valley; I = Askore Amphibolite of the Indus valley; N = Nanga Parbat – Haramosh Massif. Ar* (in nl/g) is defined as total ^{40}Ar minus total atmospheric $^{36}Ar \times 295.5$, following the usual convention. Concentrations of K and Ca (both in %) and Cl (in ppm) were calculated from the reactor-produced isotopes. All ages are in Ma, errors are 1σ. Abbreviations: $t_{K/Ar}$ integrated age (from Ar* and K), t_{pl} plateau age, t_{is} isochron age, n number of steps used to calculate plateau and isochron, f percent fraction of gas in these n steps, Ar_i trapped Ar composition, MSWD scatter of isochron fit. The scatter parameter is not defined (nd) for two-point fits.

Unit	Sample	Ar*	K	Ca	Cl	$t_{K/Ar}$	t_{pl}	n (f)	t_{is}	Ar_i	MSWD
S	B 33 amp	0.30	0.47	7.04	4	16.4	14.3 ± 1.9	6 (74)	15.3 ± 3.5	294 ± 72	2.7
S	B 33 bt	2.15	7.06	0.21	1	7.83	7.95 ± 0.20	6 (50)	8.1 ± 2.2	292 ± 127	3.0
S	C 168 amp	0.12	0.29	7.37	6	10.5	8.8 ± 2.6	7 (53)	9.2 ± 4.2	294 ± 144	1.8
S	C 168 bt	1.72	6.88	0.20	3	6.44	6.16 ± 0.09	6 (78)	6.46 ± 0.14	292 ± 8	0.19
S	C 286 amp	0.12	0.23	7.23	32	13.0	–	3 (49)	9.30 ± 1.64	288 ± 73	0.55
S	C 286 bt	7.17	6.62	0.60	29	27.7	–	–	–	–	–
I	C 342 amp	2.05	0.48	7.40	11	106.3	57.37 ± 0.12	2 (20)	55.7 ± 2.1	310 ± 28	nd
I	C 377 amp	1.98	0.82	7.91	2	61.5	–	–	–	–	–
I	C 377 bt	7.43	5.37	0.04	< 1	35.3	35.09 ± 0.07	5 (75)	34.4 ± 0.7	414 ± 108	1.3
I	C 388 amp	0.80	0.49	7.92	5	41.2	35.89 ± 0.32	2 (24)	35.4 ± 1.8	302 ± 42	nd
I	C 388 bt	10.38	7.68	0.23	2	34.5	34.14 ± 0.11	4 (26)	35.4 ± 0.1	229 ± 26	0.40
I	T 5 amp	0.50	0.35	7.68	6	36.4	36.34 ± 0.06	6 (70)	36.3 ± 0.2	295 ± 4	0.09
S	T 28 bt	1.16	5.08	0.08	2	5.90	5.76 ± 0.06	4 (38)	5.69 ± 0.25	298 ± 23	0.08
A	T 82 amp	0.79	0.39	6.76	30	51.2	–	–	–	–	–
A	T 82 bt	2.27	7.00	0.25	43	8.37	8.20 ± 0.13	8 (91)	8.20 ± 0.13	296 ± 22	6.2
N	T 88 bt	8.82	7.33	0.10	25	30.4	–	–	–	–	–
N	T 88 ms	3.99	8.27	0.06	8	12.4	11.83 ± 0.40	6 (87)	9.9 ± 0.9	415 ± 84	16
N	T 94 bt	4.70	7.43	0.05	1035	16.4	15.45 ± 0.08	4 (33)	15.2 ± 0.3	301 ± 14	0.57
N	T 94 ms	3.20	8.32	0.08	31	9.90	9.77 ± 0.20	10 (97)	8.6 ± 0.5	328 ± 36	9.3

Tab. 3 Rb/Sr data for sample T 94. Rb and Sr concentrations are in ppm, errors are 2σ. Errors on Sr ratios are referred to the last digits.

Mineral	Rb	Sr	$^{87}Rb/^{86}Sr$	$^{87}Sr/^{86}Sr$	t (Ma)	$(^{87}Sr/^{86}Sr)_0$
Bt	1411	1.6	2615.2 ± 1.6	1.06991 ± 6	5.62 ± 0.02	0.86123 ± 9
Pl	199	145	4.042 ± 0.181	0.861548 ± 44		

The muscovite gives a fairly regular spectrum, which is good evidence for a single population of undeformed muscovites, yielding an average age of 9.8 ± 0.2 Ma. The biotite has a distinctly higher isochron age of 15 Ma. To investigate the possible presence of excess Ar, we analyzed Rb/Sr on the biotite-plagioclase pair. The apparent age, 5.7 ± 0.1 Ma, confirms the presence of excess Ar but is slightly lower than the regional trend of the other $^{39}Ar/^{40}Ar$ biotite ages. In order to understand the chronological meaning beyond the numbers, it is necessary to address the assumption of isotopic equilibrium. Clearly, the biotite point alone does not provide an age and needs to be connected to another phase with which it was in isotopic equilibrium at the time of its closure. It is generally understood that the whole rock is a poor choice (GILETTI, 1991). A better choice is the phase containing most Sr and having the lowest closure temperature (450–500 °C), i.e. plagioclase. However, the use of a biotite-plagioclase two-point isochron relies both on the total absence of inherited Sr in the plagioclase and on the absence of a third phase participating in the exchange. In a polymetamorphic gneiss whose biotite incorporated excess Ar from an external source it is likely that the plagioclase underwent surface reactions with the circulating fluid (which was probably enriched in ^{87}Sr). The present-day plagioclase thus has a modified $^{87}Sr/^{86}Sr$ ratio with respect to the pristine one. Another probable explanation is that the plagioclase (whose measured $^{87}Sr/^{86}Sr$ ratio is 0.862, remarkably higher than that of comparable gneisses elsewhere in the Himalaya: FERRARA et al., 1983; DENIEL et al., 1987) indeed contains a significant inherited ^{87}Sr component. To illustrate the effects of an ^{87}Sr enrichment (be it "inherited" or fluid-transported "excess"), we can calculate the Sr initial isotopic composition the plagioclase should have if the biotite is assigned an arbitrary age; for a biotite model age of 8 Ma the plagioclase should have $^{87}Sr/^{86}Sr = 0.7731$, translating to a whole rock initial of 0.7728. Even in the extreme assumption of a plagioclase having an (unreasonably low) initial $^{87}Sr/^{86}Sr$ of 0.705, the maximum age of the biotite would be 9.8 Ma, much lower than the $^{39}Ar/^{40}Ar$ age.

We can thus summarize the age information provided by gneiss T94 as suffering from the isotopic inheritance intrinsic to polymetamorphic rock series. The muscovite $^{39}Ar/^{40}Ar$ and biotite Rb/Sr ages are consistent with the regional Tortonian (12–7 Ma) mica ages, while the biotite of this particular lithology yelds an incorrect $^{39}Ar/^{40}Ar$ age.

The two micas from the HHC gneiss *T88* show a similar age pattern as those of T94: biotite yields a 28 Ma $^{39}Ar/^{40}Ar$ age; the muscovite has an irregular spectrum suggesting an age around 11 Ma (Figs 3 c–d). By analogy with gneiss T94, we interpret the T88 biotite age as unreliable due to excess Ar. The muscovite spectrum is both less concordant and older than that of T94, which may point to excess Ar as well. As an alternative explanation it may be suggested that the older age reflects the slightly higher strucural position of sample T88 relative to T94 in the NPHM antiform.

4.2. ASKORE AMPHIBOLITE OF TURMIK VALLEY

T82 from the NW part of the AA is shown in figures 4 a–b. The amphibole has a very discordant spectrum (Fig. 4b), with step ages ranging between 29 and 72 Ma. The protolith of this rock is probably a volcanite of the Ladakh paleo-island arc of the active Eurasian paleo-margin, whose eruption age is Cenomanian or older (DIETRICH et al., 1983). This rock then was subjected to metamorphic peak temperatures of about 600–650 °C (ROLFO, 1994). This range overlaps with the temperature over which slowly cooled hornblendes retain Ar in the absence of fluid circulation (DAHL et al., 1995; KAMBER et al., 1995).

The erratic age spectrum can be interpreted by combining two separate observations. Firstly, petrography reveals a dark-brown, high-temperature (magmatic?) core with rutile needles, whose Ca/K ratio determined by microprobe is 14.7 (Tab. 1), rimmed by a clear, inclusion-free metamorphic amphibole, whose Ca/K ratio is 19.0. These two generations record two separate geological events (the Late Cretaceous magmatism, and the Himalayan amphibolite facies metamorphic over-

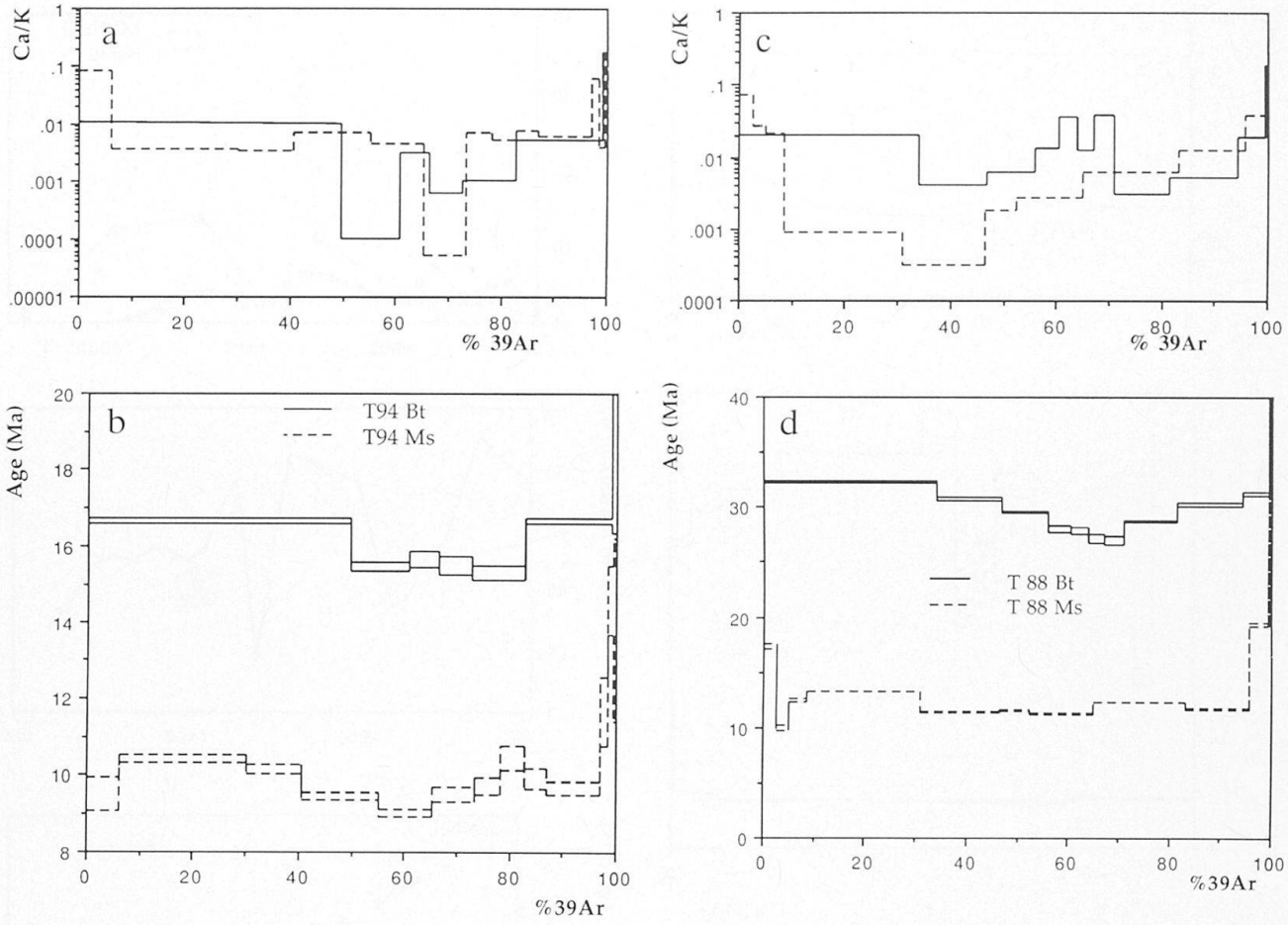

Fig. 3 $^{39}Ar/^{40}Ar$ results from NPHM. – (a, b) Ca/K and age spectrum ofT 94. – (c, d) Ca/K and age spectrum of T88.

print). Secondly, the stepwise heating data associate a Ca/K ratio with an age for every step (Figs 4 a–b).

To clarify the connection, we must briefly recall our present understanding of Ar release during in-vacuo stepwise heating. It has been demonstrated (LEE et al., 1991; WARTHO et al., 1991) that Ar is released in discrete bursts that correspond to breakdown reactions in the vacuum system. Comparing these two studies in detail, it is seen that the precise temperatures at which the discrete release bursts occur are different, and appear to reflect the chemical difference between LEE et al.'s Mg-hornblende MMhb1 and WARTHO et al.'s tschermakitic hornblende N530. This is depicted in figure 4c.

To illustrate the effects of a simple two-component mixture on the Ar release, let us consider a hypothetical sample in which MMhb1 and N530 are intergrown in such proportions that each member contributes half of the K.

When this mixture is degassed in vacuo by incremental heating, the breakdown reactions do not occur simultaneously in the two intergrown components; thus, each individual heating step carries an Ar signature dictated by the progress of breakdown reactions at that particular temperature. Figure 4d shows the percentage of the Ar release that derives from MMhb1 at a given temperature. It can be seen that MMhb1 dominates the release at different temperatures than N530, allowing a surprisingly good separation of the two pure end-members (e.g the 930 °C step consists by 91% of MMhb1 gas, and the 1060 °C step consists by 84% of N530 gas).

These last two graphs are impractical to use in that they are based on a perfect knowledge of the degassing characteristic of each end-member of the mixture. A more convenient approach is displaying the apparent step ages against some chemical information provided by the Ar of that same step. In this way, electron microprobe analyses can be invoked to constrain the end-members and used to estimate the degree to which end-member separation was effective. The chemical elements monitored by Ar isotopes are K, Cl and Ca, and in most minerals the Ca/K ratio is known most accurately among the possible combinations of these elements. Figure 4e shows the Ca/K vs age

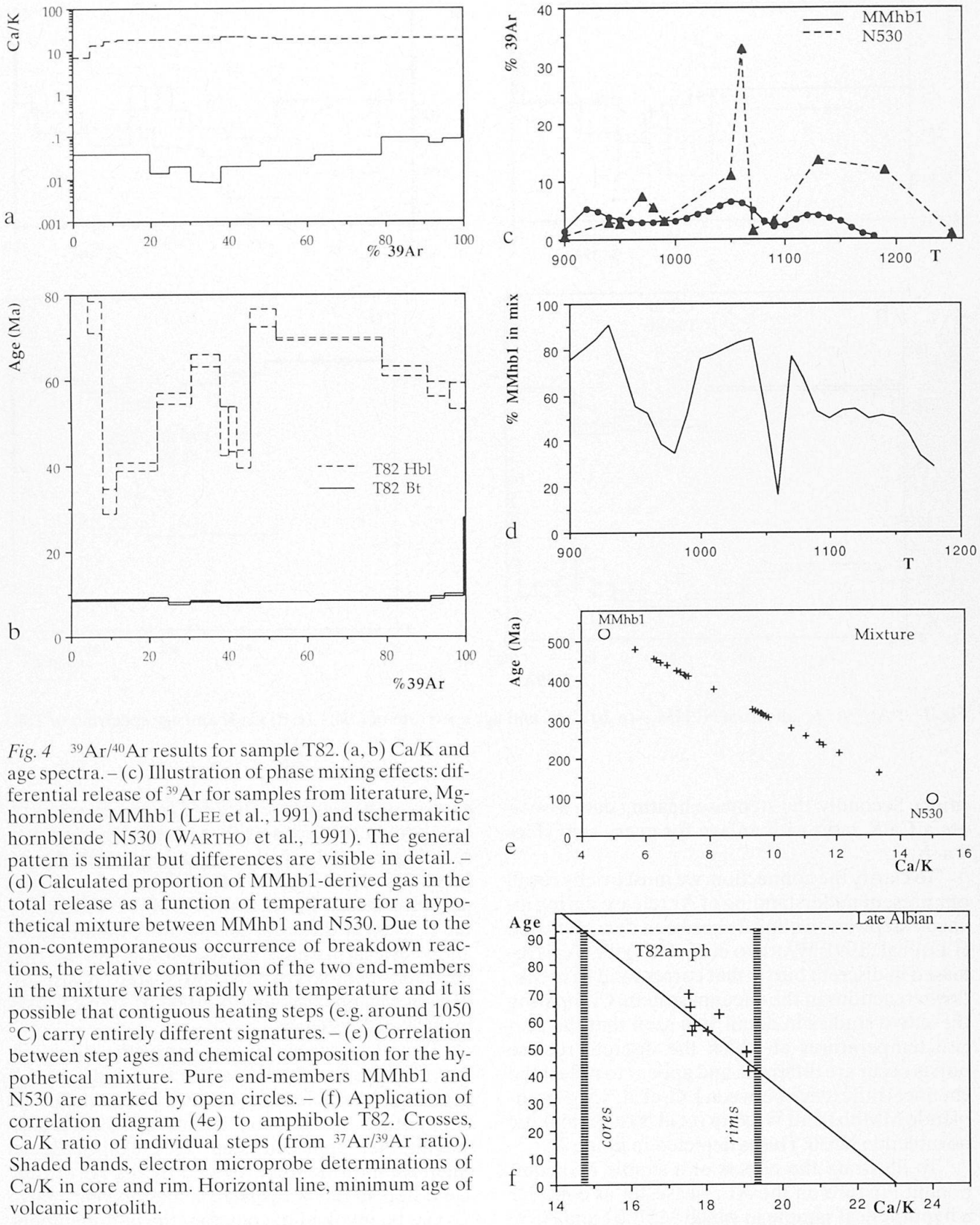

Fig. 4 $^{39}Ar/^{40}Ar$ results for sample T82. (a, b) Ca/K and age spectra. – (c) Illustration of phase mixing effects: differential release of ^{39}Ar for samples from literature, Mg-hornblende MMhb1 (LEE et al., 1991) and tschermakitic hornblende N530 (WARTHO et al., 1991). The general pattern is similar but differences are visible in detail. – (d) Calculated proportion of MMhb1-derived gas in the total release as a function of temperature for a hypothetical mixture between MMhb1 and N530. Due to the non-contemporaneous occurrence of breakdown reactions, the relative contribution of the two end-members in the mixture varies rapidly with temperature and it is possible that contiguous heating steps (e.g. around 1050 °C) carry entirely different signatures. – (e) Correlation between step ages and chemical composition for the hypothetical mixture. Pure end-members MMhb1 and N530 are marked by open circles. – (f) Application of correlation diagram (4e) to amphibole T82. Crosses, Ca/K ratio of individual steps (from $^{37}Ar/^{39}Ar$ ratio). Shaded bands, electron microprobe determinations of Ca/K in core and rim. Horizontal line, minimum age of volcanic protolith.

correlation for the hypothetical MMhb1-N530 mixture, calculated from the respective chemical compositions and from the relative contributions to step gas (Fig. 4d). Irrespective of the temperature sequence, the data points define a mixing line approaching the pure end-members.

This correlation diagram is now applied to the T82 stepwise heating data (Fig. 4f).

The figure also shows additional independent constraints such as the minimum stratigraphic age of the LT magmatism and the electron microprobe values of the Ca/K ratio measured on amphibole rims and cores. It can be seen that the spread among the data points allows to calculate a correlation line. The interceptions of this correlation line with the vertical bands representing the chemical composition of the pure end-members is a reasonable estimate of the age of the cores (≈ 100 Ma, supporting the suggestion that the cores have a magmatic origin) and the amphibolite-facies overgrowths (≈ 35–40 Ma).

Thus, the "old cores" of the T82 hornblendes preserve a large part of their accumulated Ar, almost unaffected by the Eocene amphibolite metamorphism (600–650 °C). The discordant step ages derive from mixing a weakly disturbed Cretaceous Ar signature with a heterochemical Eocene overgrowth, and certainly cannot be attributed to laboratory deconvolution of an Ar zoning produced by diffusion.

The biotite of sample T82 has a comparatively regular spectrum. Step ages define no statistically acceptable plateau, but have a very limited variation range from 7.7 to 8.8 Ma (Fig. 4b). The average "pseudo-plateau" age of 8.2 ± 0.1 Ma can be taken as the biotite cooling age. This age is remarkably close to the mica ages from the "Layered Series" of the NPHM in the Stak valley, T88 and T94 (see above) but much younger than the Oligocene ages of the AA micas from the Indus valley (see below). This likely indicates the geographical extent of the Tortonian tectonometamorphism.

4.3. ASKORE AMPHIBOLITE OF THE INDUS VALLEY

Sample *T5* is shown in figures 5 a–b. Its age spectrum allows a fairly straightforward interpretation: all age steps with Ca/K ≥ 24.6, i.e. those most likely to derive from the hornblende sensu stricto (which account for 70% of the Ar release), define a statistically flawless isochron (Tab. 2) and a plateau at 36.34 ± 0.06 Ma. While the field relations would not rule out that the age of this sample mirrors the contact metamorphism from the intruding Ladakh pluton, such a regular age spectrum makes it more likely that 36.3 Ma is the age of the amphibolite facies metamorphism (or cooling to ≈ 600–650 °C immediately following it).

Sample *C342* is also shown in figures 5 a–b. The age spectrum is apparently quite different from that of T5. However, it can be noted that there is a sympathetic behaviour of the Ca/K ratio and the step ages (a similar pattern as T82, but in the other direction). The three oldest step ages, corresponding to Ca/K ratios of > 21.1 and accounting for 12% of the Ar, average 105 Ma, an age which may well be a genuine remnant of the Cretaceous arc magmatism. Four other steps with lower Ca/K have step ages between 57 and 70 Ma; as the relationship between Ca/K and ages is not as regular as in T82, it is impossible to decide whether 57 Ma (the lowest step age) should be interpreted as the age of an "end-member amphibole" entirely formed during a Paleocene amphibolite-facies event, or as a mixture between an Eocene recrystallization and a Cretaceous relic. Interpretation as a purely thermal overprint of the Cretaceous amphibole is unlikely because the Ca/K-age parallelism shows the presence of at least 2 phases.

Biotite and amphibole *C377* are shown in figures 5 c–d. The biotite yields a well-defined isochron (Tab. 2) and a plateau age of 35.09 ± 0.07 Ma, surprisingly close to the hornblende plateau age of T5. In contrast, the hornblende age spectrum is quite erratic, and no regular correlation between age and Ca/K ratio can be recognized.

Biotite *C388* also yields a well-defined isochron (Tab. 2), with a plateau age slightly younger than C377, 34.14 ± 0.11 Ma (Figs 5 e–f). The coexisting hornblende shows a weak parallelism between step ages and Ca/K ratios. More importantly, the youngest step ages are indistinguishable, at the 2-sigma level, from the plateau age of T5 (Tab. 2), and only about 1 Ma older than biotites C377 and C388. The proximity of amphibole and biotite ages leads us to interpret the 35.9 Ma age of the C388 hornblende as that of an "end-member amphibole" formed during the (fairly rapid) Eocene amphibolite facies metamorphism.

None of these four samples show any evidence of a Miocene overprint.

4.4. SHYOK SUTURE ZONE

Sample *B33* is shown in figures 6 a–b. The amphibole yields an unambiguous Miocene age (14.3 ± 1.9 Ma). Since the amphibole appears both petrographically and compositionally to be a homogeneous, single-generation phase, it is probable that this age represents the amphibolite facies meta-

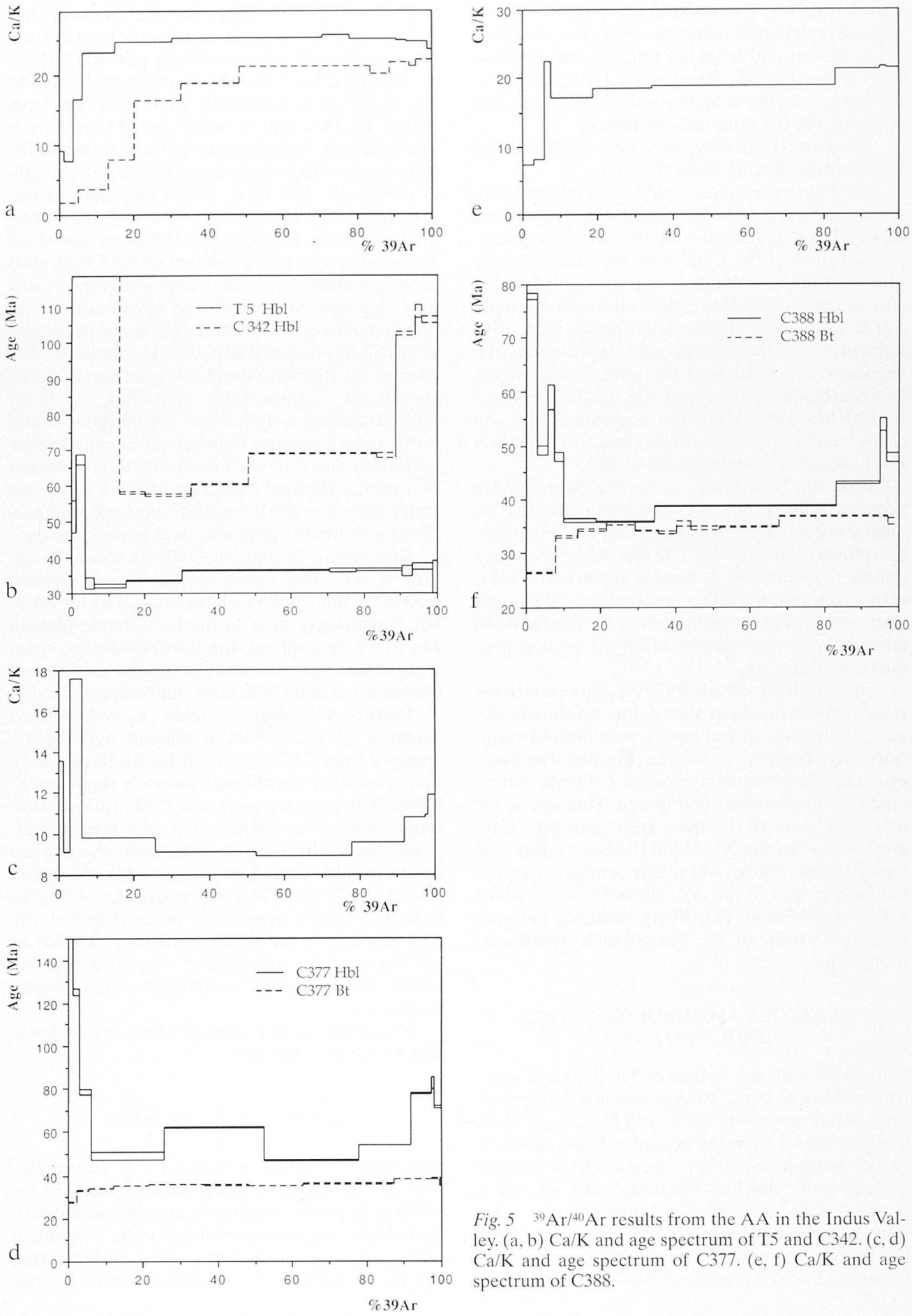

Fig. 5 $^{39}Ar/^{40}Ar$ results from the AA in the Indus Valley. (a, b) Ca/K and age spectrum of T5 and C342. (c, d) Ca/K and age spectrum of C377. (e, f) Ca/K and age spectrum of C388.

morphism, or closely approaches it (cfr. sample T5 above). The biotite spectrum strongly resembles that of T82; its "pseudo-plateau" age is 7.9 ± 0.1 Ma.

Sample *C168* is shown in figures 6 c–d. The amphibole gives a "pseudo-plateau" age of 8.8 ± 2.6 Ma. This young amphibole age translates into a nominal cooling rate if one makes the assumption that this sample remained dry and undeformed after the thermal climax. In that case, a temperature drop of 625 ± 25 K was completed in 8.8 ± 2.6 Ma, i.e. at an average rate of 71 ± 21 K/Ma. The biotite has a statistically flawless plateau age of 6.25 ± 0.07 Ma.

These well-behaved spectra are associated with the highest PT conditions experienced by this sample. This observation may be interpreted if in C168 both amphibole and biotite were recrystallized statically, i.e. deformation was completed before these minerals began to retain Ar. This means that C168 may be considered to record a purely thermostatic cooling age; only in this case is it legitimate to use the concept of closure temperature. For rapidly cooled biotite (50 K/Ma) it is 450 °C (VILLA and PUXEDDU, 1994). The average cooling rate from 6.25 Ma to now, 72 K/Ma, is identical to that estimated from the amphibole age (see above). Note that even higher Mio-Pliocene cooling rates have been reported from the NPHM (ZEITLER, 1985).

The age difference between the two hornblende-biotite chronometer pairs from SSZ discussed above is variable. This should not blindly be extrapolated into a variation of cooling rates: firstly, there is a dependence of retentivity on composition (DAHL et al., 1995); secondly, the extent to which hornblendes and biotites were locally affected by fluid circulation and temperature-independent rejuvenation is at present unknown.

From sample *C286*, biotite and hornblende were analyzed (Figs 6 e–f). The hornblende age spectrum is irregular, but a statistically acceptable isochron of 9.3 ± 1.6 Ma is obtained. This age is indistinguishable from that of C168. The biotite has a very irregular spectrum (Fig. 6f), and no isochron can be calculated. The integrated K/Ar age (27.7 Ma) is much higher than the hornblende age and clearly points to excess Ar.

Biotite *T28* is shown in figure 6g. Its age spectrum features a staircase shape, suggestive of a two-phase mixture; the variation band of the step ages is ≈ 0.6 Ma, and a reasonable estimate of its age, ≈ 5.7 Ma (Tab. 2), is close to that of C168 biotite.

5. Discussion

Radiometric ages for the LT and SSZ in Baltistan are scarce. A Rb/Sr date of about 49.6 Ma was obtained by DESIO et al. (1964) on the undeformed Satpura granodiorite of the Ladakh-Deosai batholith south of Skardu, ≈ 50 km SE of our field area. A $^{39}Ar/^{40}Ar$ age of about 42 Ma was obtained by BROOKFIELD and REYNOLDS (1981) on a muscovite from an unaltered dacite dike intruding amphibolite-facies metasediments marginal to the Satpura granodiorite. Similar ages of 44.0 ± 0.5 Ma and 39.7 ± 0.2 Ma were obtained by REYNOLDS et al. (1983) on biotite from a pegmatite and hornblende from a foliated diorite at Khaplu, 50 km east of Skardu. This would imply that amphibolite conditions had ceased, and exhumation to upper crustal levels occurred, by 44 Ma. Two zircon fission-track ages from the Skardu region (ZEITLER, 1985), one from the Satpura granodiorite and one from a granodiorite at the western end of Skardu basin are 24.4 ± 2.0 and 15.4 ± 1.3 Ma, whilst apatite FT ages from the same samples (11.1 ± 2.4 Ma and 8.2 ± 1.7, respectively) date cooling to ≈ 100 °C.

As shown in the compilation by TRELOAR et al. (1991, Fig. 10) mica and fission track ages in the NPHM along the Indus gorge transect are very young, ranging between 3.1 and 9.5 Ma for biotite, 3.1–7.0 Ma for muscovite, 1.7–5.3 Ma for zircon, and 0.39–1.30 Ma for apatite. ZEITLER and CHAMBERLAIN (1991) report SHRIMP U/Pb analyses of zircons from three leucogranite dykes cross-cutting the Shengus and Iskere gneisses in the Indus River, and obtain average ages between 2.3 and 13 Ma. In the area to the N of the Indus River (Jutial and Iskere valleys) GEORGE and BARTLETT (1996) report reset mica ages (not to be confused with "cooling" ages) between 2 and 7 Ma, reflecting rejuvenation by very intense fluid circulation during deformation. This implies that exhumation of the NPHM was actively proceeding around Late Miocene-Pliocene.

In the Chogo Lungma-Turmik area, the age of the deformation that produced the regional foliation both in the "Layered Sequence" of the NPHM and in the overlying amphibolites is unknown, but it certainly predates the phase of doming in the KMC and in the NPHM and the emplacement of the Remendok leuco-trondhjemite at 8.3 Ma, after which the MMT became inactive (VILLA et al., 1996). These authors also proposed that exhumation along the MKT in the Eurasian plate, together with deformation of the metamorphics in its hanging wall, took place from about 10 Ma and was associated with emplacement of cross-cutting igneous bodies, the contact aureole

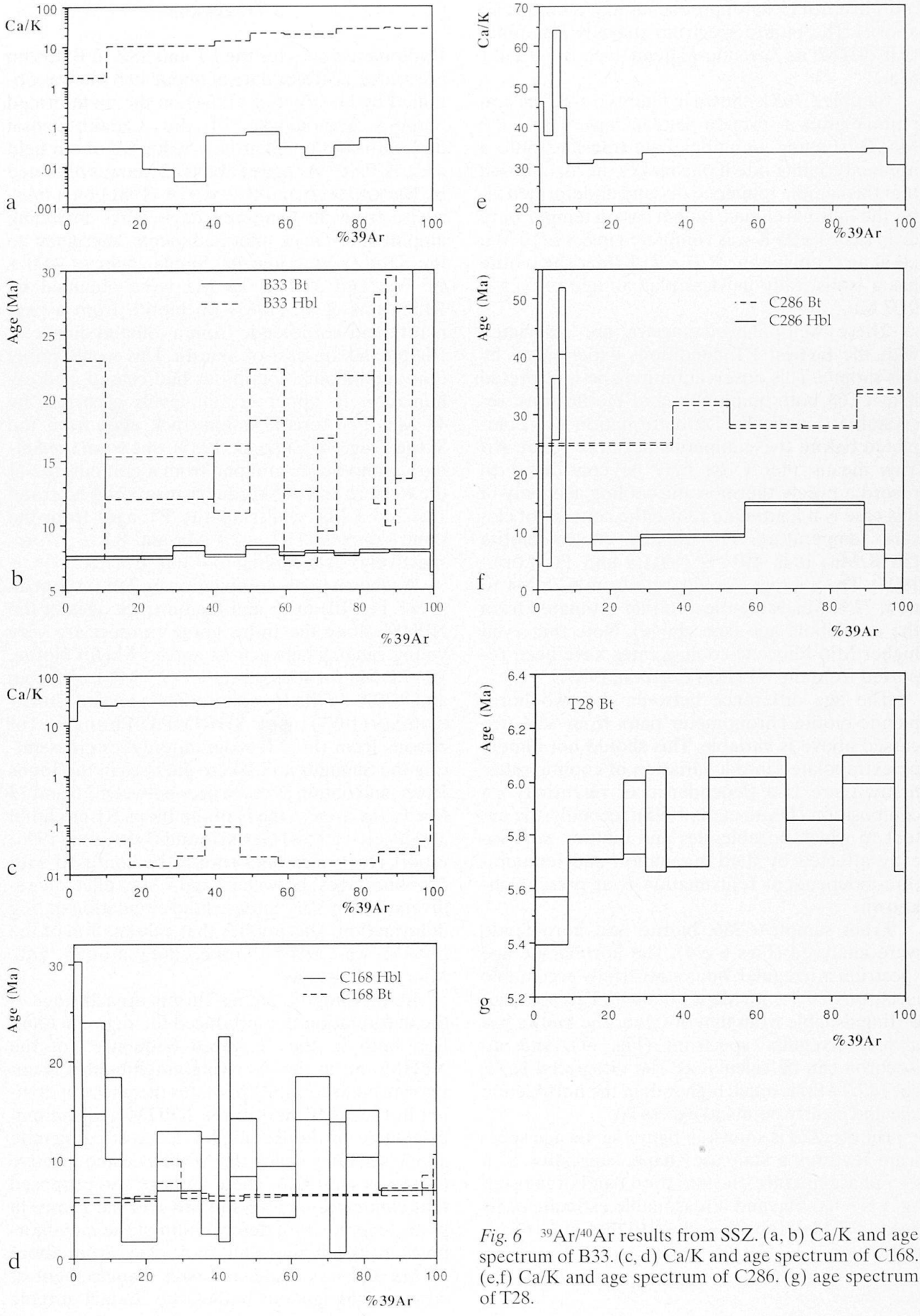

Fig. 6 $^{39}Ar/^{40}Ar$ results from SSZ. (a, b) Ca/K and age spectrum of B33. (c, d) Ca/K and age spectrum of C168. (e,f) Ca/K and age spectrum of C286. (g) age spectrum of T28.

of one of which (the Hemasil Syenite) has yielded a hornblende age as young as 5.5 Ma.

Young mineral ages have also been obtained in the KMC, in the area from Braldu valley to the Baltoro Glacier. Specifically, K–Ar ages of 4.69 ± 0.19, 7.10 ± 0.28 and 7.0 ± 0.3 Ma were obtained by SEARLE et al. (1989) on biotite from two samples of Dassu gneiss and on muscovite from a marble west of Dassu, respectively. These authors also report biotite and muscovite K–Ar ages from pegmatite and granite dikes emplaced in the KMC exposed further east, between the Panmah river and Paiyu, at the mouth of Baltoro glacier, which range between 5.87 ± 0.20 Ma (biotite, Panmah river) and 8.8 ± 0.3 Ma (muscovite, Bardumal migmatite). SEARLE et al. (1989) attributed these ages to thermal reequilibration along the hanging wall of the MKT. The spatial distribution of these ages suggests that they are structurally controlled, with the youngest cooling ages recorded in the structurally deepest parts of the KMC.

Our results allow to better place the scarce available data base in a regional perspective. We document the existence of two discrete amphibolite facies events (with different P/T ratios) in the LT and the SSZ.

Ages of LT rocks in the Indus valley, far from the syntaxis, are Late Eocene or older, and only record the first (Eocene, higher P/T) event. In the SSZ of the Chogo Lungma-Turmik area, all mineral ages are Late Miocene and show no indication of Eocene relics, suggesting that only one generation of (lower P/T) amphibolite facies minerals was ever formed. Towards the NPHM, one biotite from the AA (sample T82) has been reequilibrated, yielding an 8.2 Ma age, but the amphibole still records the Eocene event. In conclusion, the most intense recent tectonic activity and exhumation are found in the Shyok Suture Zone close to the Karakorum Metamorphic Complex and in the Askore Amphibolite located just above the MMT and the NPHM, i.e. towards the area where the Nanga Parbat indenture comes nearest to Karakorum and the Ladakh Terrain is most thinned out. The rapid rate of uplift (and hence of exhumation) within the north-western tip of LT is also indicated by the dramatic form of the topography in the Haramosh-Chogo Lungma region, and by the deeply incised nature of the drainage system cutting both the Karakorum and the NPHM. By contrast, the topography over the region where only Eocene tectonometamorphism was present, the Ladakh-Deosai batholith, is subdued (Deosai Plains) and elevations are significantly lower than in both the Karakorum and the NPHM.

A change in the mechanism accommodating the India-Asia convergence may have occurred in the Late Miocene. LEE and LAWVER (1995) note a change in direction of the relative movement of India and Asia at 10 Ma, which they attribute to "anchoring in the Hindu Kush" (ibid., Fig. 17). It appears remarkable that this change of direction occurred at the same time as doming and vertical extrusion of the KMC and NPHM and the locking of the Main Mantle Thrust (VILLA et al., 1996) and the prograde burial of the Shyok Suture Zone.

6. Conclusions

The Askore Amphibolite (metavolcanic rocks of the Ladakh Terrain in NW Baltistan which are a correlative of the Chalt volcanics of the Kohistan Terrain) records amphibolite facies metamorphism and diachronous cooling. In the Turmik-Chogo Lungma area, peak conditions were 10 kbar, 600–650 °C in the north-west, near the Nanga Parbat-Haramosh Massif, and 5–6 kbar, 600–650 °C further south-east in the Indus valley halfway between Skardu and Rondu. NPHM rocks from the "Layered Sequence" of the Stak valley and Chogo Lungma Glacier record garnet-granulite conditions, with an early compressional evolution from the sillimanite to the kyanite stability field, a metamorphic peak at T = 650–700 °C and P = 12–15 kbar, followed by decompressional cooling in the kyanite field.

$^{39}Ar/^{40}Ar$ age spectra of several of our samples display internal discordances that are probably due to the deformational history, which in the LT and Shyok Suture Zone was concluded by (locally incomplete?) static recrystallization of amphibole and biotite porphyroblasts. Most age spectra are not perfectly flat, nor Ca/K spectra strictly monotonic. The systematics of mineral chronometers could be assessed by virtue of the numerous cross-checks between samples. Amphiboles generally display apparently complex spectra, which at least in one case can be interpreted in terms of petrographically observed core overgrowths. Old amphibole cores retain their Ar even at high metamorphic temperatures (600–650 °C). Biotites from the NPHM contain excess Ar, but yield $^{39}Ar/^{40}Ar$ age spectra and isochrons which simulate near-ideal behaviour. The Rb/Sr system of one biotite-plagioclase pair also gives an apparent age which may be too young because of fluid circulation and/or ^{87}Sr inheritance in plagioclase.

Still, despite the complexities of individual samples, combining structural field observations with P-T estimates allows to interpret age data in a general picture: in the Ladakh Terrain, the Askore Amphibolite experienced an amphibolitic

event, probably around 35–40 Ma, which was followed by contrasting exhumation styles: in the Indus valley, biotite ages are very close to hornblende ages, indicating a rapid evolution; in one AA sample from the NW, isotopic closure of biotite occurred at 8.2 Ma, reflecting an amphibolite facies Late Miocene overprint during underthrusting of the NPHM. The Shyok Suture Zone far from the syntaxis consists of greenschist facies rocks. Approaching MKT we observed an increase in metamorphic grade, which we attribute to thermal overprinting along the footwall of the MKT. The new amphiboles of the SSZ close to the Karakorum Metamorphic Complex document a pressure increase during their formation, suggesting that amphibolite facies metamorphism of the preexisting greenschist lithologies occurred during, and because of, the thrusting of KMC over SSZ in the Tortonian (≈ 10 Ma). SSZ mineral ages of amphibolite facies rocks are all Late Miocene.

Within the LT, $^{39}Ar/^{40}Ar$ ages are older, and the peak pressures lower toward the interior of the LT than toward the contacts with NPHM and KMC. The average exhumation rate at the NW tip of the LT was extremely high during the last 10 Ma. This fast exhumation has resulted in mineral deformation and recrystallization along the MMT (sample T82), whereas "thermostatic" cooling is probably found in sample T94 from the innermost part of the NPHM and in medium-grade lithologies of SSZ (C168, B33), which give a very high rate of post-metamorphic cooling (70 K/Ma).

As a final conclusion, we note that mapping and sampling on a closer scale than in previous reconnaissance work has substantially widened the extent of the area in north-western Himalaya where Tortonian-Pliocene exhumation of deep-seated metamorphic and plutonic rocks has been documented.

Acknowledgements

Fieldwork in the Chogo Lungma-Turmik area was financially supported by EEC contract n° CT1 CT 90/0852. Samples "T" were collected in 1991 by the late U. Pognante, together with P. Benna and P. Le Fort. M. Oddone is thanked for the neutron irradiations in Pavia. J.D. Kramers is thanked for encouragement, discussion, and help with the Rb/Sr measurement. The manuscript benefitted from constructive criticism by P. Treloar and J.-P. Burg. Laboratory work by B.L. and F.R. has been funded by C.S. Geodinamica Catene Collisionali, CNR, and Dipartimento di Scienze Mineralogiche e Petrologiche, Università di Torino. The Bern Isotope Laboratory is funded by the Schweizerische Nationalfonds zur Förderung der wissenschaftlichen Forschung, grant 20-40442.94.

References

Allen, T. and Chamberlain, C.P. (1991): Metamorphic evidence for an inverted crustal section, with constraints on the Main Karakorum Thrust, Baltistan, N Pakistan. J. Metam. Geol. 9, 403–418.

Bard, J.P., Maluski, H., Matte, P. and Proust, F. (1980): The Kohistan sequence: crust and mantle of an obducted island arc. Proc. Intern. Commit. Geodyn. Grp. 6 Meeting, Peshawar. Spec. Issue, Geol. Bull. Univ. Peshawar, Vol. 13.

Butler, R.W.H., George, M.T., Harris, N.B.W., Jones, C., Prior, D.J., Treloar, P.J. and Wheeler, J. (1992): Geology of the northern part of the Nanga-Parbat massif, northern Pakistan, and its implications for Himalayan tectonics. J. Geol. Soc. London, 149, 557–567.

Brookfield, M.E. and Reynolds, P.H. (1981): Late Cretaceous emplacement of the Indus Suture zone ophiolitic mélanges and an Eocene-Oligocene magmatic arc on the northern edge of the Indian Plate. Earth Planet. Sci. Lett., 55, 157–162.

Casnedi, R. and Ebblin, C. (1977): Geological notes on the area between Astor and Skardu (Kashmir). Acc. Naz. Lincei, Rend. Sc. fis. mat. nat., LXII, 662–668.

Coward, M.P., Windley, B.F., Broughton, R.D., Luff, I.W., Petterson, M.G., Pudsey, C.J., Rex, D.C. and Asif Khan, M. (1986): Collision Tectonics in the NW Himalayas, Collision Tectonics, Geol. Soc. Spec. Publ. 19, 203–219.

Dahl, P.S., Kamber, B.S. and Villa, I.M. (1995): Field evidence of crystal fields: the diffusivity-composition link in hornblende. Terra Abstr., 7, 289–290.

Deniel, C., Vidal, P., Fernandez, A., Le Fort, P. and Peucat, J.J. (1987): Isotopic study of the Manasly granite (Himalaya, Nepal): inferences on the age and source of the Himalayan leucogranites. Contrib. Mineral. Petrol. 96, 78–92.

Desio, A. (1963): Review of the geologic formations of the western Karakorum (Central Asia). Riv. It. Paleont. 59, 475–501.

Desio, A. (1978): On the geology of the Deosai plateau (Kashmir). Atti Accad. Naz. Lincei, Mem. Ser. VIII, 15, 1–19.

Desio, A., Tongiorgi, E. and Ferrara, G. (1964): Notizie preliminari sull'età geologica di alcune rocce granitoidi del Karakorum, Hindu Kush e Badakhshan (Asia Centrale). Rend. Acc. Naz. Lincei, 8, XXXVI, 6, 776–783.

Dietrich, V.J., Frank, W. and Honegger, K. (1983): A Jurassic-Cretaceous island arc in the Ladakh-Himalayas. J. Volc. Geotherm. Res., 18, 405–433.

Ferrara, G., Lombardo, B. and Tonarini, S. (1983): Rb/Sr geochronology of granites and gneisses from the Mt. Everest region, Nepal Himalaya. Geol. Rundsch., 72, 119–136.

George, M.T. and Bartlett, J.M. (1996): Isotopic constraints on differential uplift on the margin of the Nanga Parbat-Haramosh Massif. Tectonophysics, in press.

Giletti, B.J. (1991): Rb and Sr diffusion in alkali feldspars, with implications for cooling histories of rocks. Geochim. Cosmochim. Acta, 55, 1331–1343.

Greco, A., Martinotti, G., Papritz, K., Ramsay, J.G. and Rey, R. (1989): The crystalline rocks of the Kaghan Valley (NE Pakistan). Eclogae geol. Helv. 82, 629–653.

Hanson, C.R. (1989): The northern suture in the Shigar valley, Baltistan, northern Pakistan. Geol. Soc. Amer. Spec. Pap., 232, 203–215.

HODGES, K.V. and CROWLEY, P.D. (1985): Error estimation and empirical geothermobarometry for pelitic systems. Amer. Mineral., 70, 702–709.

HODGES, K.V. and SPEAR, F.S. (1982): Geothermometry, geobarometry and the Al_2SiO_5 triple point at Mt. Moosilauke, New Hampshire, Amer. Mineral. 67, 1118–1134.

HOLLAND, T.J.B. (1980): The reaction albite = jadeite + quartz determined experimentally in the range 600–1200 °C. Amer. Mineral. 65, 129–134.

INDARES, A. and MARTIGNOLE, J. (1985): Biotite-garnet geothermometry in the granulite facies: the influence of Ti and Al in biotite. Amer. Mineral. 70, 272–278.

KAMBER, B.S., BLENKINSOP, T.G., VILLA, I.M. and DAHL, P.S. (1995): Proterozoic transpressive deformation in the Northern Marginal Zone, Limpopo Belt, Zimbabwe. J. Geol. 103, 493–508.

KHAN, T. (1994): Back-arc basin assemblages in Kohistan, Himalaya, North Pakistan. Ph. D. thesis, Univ. Peshawar, 250 pp.

KOZIOL, A.M. and NEWTON, R.C. (1988): Redetermination of the anorthite breakdown reaction and improvement of the plagioclase – garnet – Al_2SiO_5 – quartz geobarometer. Amer. Mineral. 73, 216–223.

KRETZ, R. (1983): Symbols for rock-forming minerals. Amer. Mineral. 68, 277–279.

KROGH, E. J. (1988): The garnet-clinopyroxene Fe–Mg geothermometer – a reinterpretation of existing experimental data. Contrib. Min. Petr. 99, 44–48.

LE FORT, P., LEMENNICIER, Y., LOMBARDO, B., PÊCHER, A., PERTUSATI, P., POGNANTE, U. and ROLFO, F. (1995): Preliminary geological map and description of the Himalaya-Karakorum junction in Chogo Lungma to Turmik area (Baltistan, northern Pakistan). J. Geol. Soc. Nepal 11, 17–38.

LEAKE, B.E. (1978) Nomenclature of Amphiboles. Amer. Mineral. 63, 1023–1052.

LEE, J.K.W., ONSTOTT, T.C., CASHMAN, K.V., CUMBEST, R.J. and JOHNSON, D. (1991): Incremental heating of hornblende in vacuo: Implications for $^{40}Ar/^{39}Ar$ geochronology and the interpretation of thermal histories. Geology 19, 872–876.

LEE, T.Y. and LAWVER, L.A. (1995): Cenozoic plate reconstruction of Southeast Asia. Tectonophysics 251, 85–138.

LEMENNICIER, Y., LE FORT, P., LOMBARDO, B., PÊCHER, A. and ROLFO, F. (1995): Tectonometamorphic evolution of the central Karakorum (Baltistan – Northern Pakistan). Abstract, 10th Himalaya-Karakorum-Tibet workshop, Ascona.

LOMBARDI, F. (1991): Geodetic and Topographic survey of Desio's 1954 expedition. Italian expeditions to the Karakorum (K2) and Hindu Kush Scientific Reports, vol. I, part 21.

MADIN, I.P. (1986): Structure and neotectonics of the north-western Nanga Parbat-Haramosh massif. MSc. Thes., Oregon St. Univ., 160 pp.

NEWTON, R.C. and HASELTON, H.T. (1981): Thermodynamics of the garnet-plagioclase – Al_2SiO_5 – quartz geobarometer. In: NEWTON, R.C., NAVROTSKY, A. and WOOD, B.J. (eds): Thermodynamics of Minerals and Melts. Springer-Verlag, New York, 129–145.

NEWTON, R.C. and PERKINS, D. (1982): Thermodynamic calibration of geobarometers based on the assemblages garnet-plagioclase-orthopyroxene (clinopyroxene)-quartz. Amer. Mineral. 67, 203–222.

PERCHUK, L.L. and LAVRENT'EVA, I.V. (1983): Experimental investigation of exchange equilibria in the system cordierite-garnet-biotite. In: SAXENA, S.K. (ed.): Kinetics and Equilibrium in Mineral Reactions, Springer-Verlag, New York, 199–239.

PETTERSON, M.G., WINDLEY, B.F. and SULLIVAN, M. (1991): A petrological, chronological, structural and geochemical review of Kohistan batholith and its relationship to regional tectonics. Geology and geodynamic evolution of the Himalayan collision zone, Wadia Inst. Himalayan Geology, part II, 47–70.

POGNANTE, U., BENNA, P. and LE FORT, P. (1993): High-pressure metamorphism in the High Himalayan Crystallines of the Stak valley, north-eastern Nanga Parbat-Haramosh syntaxis, Pakistan Himalaya. Himalayan Tectonics, Geol. Soc. Spec. Publ., 74, 161–172.

POWELL, R. (1985): Regression diagnostics and robust regression in geothermometer / geobarometer calibration: the garnet-clinopyroxene geothermometer revisited. J. Metam. Geol. 3, 231–243.

POWELL, R. and HOLLAND, T.J.B. (1988): An internally consistent thermodynamic dataset with uncertainties and correlations: 3. Applications to geobarometry, worked examples and a computer program. J. Metam. Geol. 6, 173–204.

RAASE, P. (1974): Al and Ti contents of hornblende, indicators of pressure and temperature of regional metamorphism. Contr. Mineral. Petrol. 45, 231–236.

REYNOLDS, P.H., BROOKFIELD, M.E. and MCNUTT, R.H. (1983): The age and nature of the Mesozoic-Tertiary magmatism across the Indus suture in Kashmir and Ladakh (NW India and Pakistan). Geol. Rundsch. 73, 981–1004.

ROLFO, F. (1994): Studio Geologico-Petrografico dei terreni compresi tra Himalaya e Karakorum nella regione ad est della Sintassi Haramosh-Nanga Parbat (Baltistan, Pakistan Settentrionale). MSc. Thesis, Univ. Torino, 130 pp.

ROLFO, F., COMPAGNONI, R., LE FORT, P., LEMENNICIER, Y., LOMBARDO, B. and PÊCHER, A. (1995): Metamorphic evolution of the NE Nanga Parbat-Haramosh Massif and of the Ladakh Terrain in the Chogo Lungma-Turmik area (Northern Pakistan). Abstract, 10th Himalaya-Karakorum-Tibet workshop, Ascona.

SEARLE, M.P., REX, A.J., TIRRUL, R., REX, D.C., BARNICOAT, A. and WINDLEY, B.F. (1989): Metamorphic, magmatic, and tectonic evolution of the central Karakorum in the Biafo-Baltoro-Hushe regions of northern Pakistan. Geol. Soc. Amer. Spec. Paper 232, 47–73.

TAHIRKHELI, R.A.K., MATTAUER, M., PROUST, F. and TAPPONNIER, P. (1979): The India-Eurasia suture zone in northern Pakistan; some new data for an interpretation at plate scale. Geodynamics of Pakistan, Geol. Surv. Pakistan, Quetta, 125–130.

THAKU, V.C. (1993): Geology of Western Himalaya. Phys. Chem. Earth, 19, 1–366.

TRELOAR, P.J., POTTS, G.J., WHEELER, J. and REX, D.C. (1991): Structural evolution and asymmetric uplift of the Nanga Parbat syntaxis, Pakistan Himalaya. Geol. Rundsch. 80, 411–428.

VERPLANCK, P.C. (1986): A field and geochemical study of the boundary between the Nanga Parbat-Haramosh Massif and the Ladakh Arc Terrane, northern Pakistan. MSc. Thesis, Oregon State University, 135 pp.

VERPLANCK, P.C., SNEE, L.W. and LUND, K. (1985): The boundary between the Nanga Parbat massif and Ladakh island arc terrain, northern Pakistan; a cross fault on the Main Mantle Thrust. EOS, 66, 1074.

VILLA, I.M., LEMENNICIER, Y. and LE FORT, P. (1996): Late Miocene to Early Pliocene tectonometamor-

phism and cooling in south-central Karakorum and Indus-Tsangpo suture, Chogo Lungma area (NE Pakistan). Tectonophysics, in press.

VILLA, I.M. and PUXEDDU, M. (1994): Geochronology of the Larderello geothermal field: new data and the "closure temperature" concept. Contrib. Mineral. Petrol. 115, 415–426.

WARTHO, J.A., DODSON, M.H., REX, D.C. and GUISE, P.G. (1991): Mechanisms of Ar release from Himalayan metamorphic hornblende. Amer. Mineral. 76, 1446–1448.

WHEELER, J., TRELOAR, P.J. and POTTS, G.J. (1991): Structural and metamorphic evolution of the Nanga Parbat syntaxis, Pakistan Himalayas, on the Indus gorge transect: the importance of early events. Geological J. 30, 349–371.

ZAKRUTKIN, V.V. (1968): The evolution of amphiboles during metamorphism. Zap. Yses. Mineral. Obsch. 96, 13–23.

ZANETTIN, B. (1964): Geology and Petrology of Haramosh-Mango Gusor Area. Italian expeditions to the Karakorum (K2) and Hindu Kush Scientific Reports. III. Brill, Leiden, 305 pp.

ZEITLER, P.K. (1985): Cooling history of the NW Himalaya, Pakistan. Tectonics, 4, 127–151.

ZEITLER, P.K. and CHAMBERLAIN, C.P. (1991): Petrogenetic and tectonic significance of young leucogranites from the northwestern Himalaya, Pakistan. Tectonics 10, 729–741.

ZEITLER, P.K., SUTTER, J.F., WILLIAMS, I.S., ZARTMAN, R. and TAHIRKHELI, R.A.K. (1989): Geochronology and temperature history of the Nanga Parbat-Haramosh massif, Pakistan. Geol. Soc. Amer. Spec. Pap., 232, 1–22.

Manuscript received October 12, 1995; revision accepted May 12, 1996.